

Single-Molecule Magnets

Unusual Magnetic Metal–Cyanide Cubes of Re^{II} with Alternating Octahedral and Tetrahedral Corners**

Eric J. Schelter, Andrey V. Prosvirin, William M. Reiff, and Kim R. Dunbar*

The design of cyanide-bridged transition-metal clusters is one of the leading topics in the field of molecular magnetism.^[1] Two of the main reasons for this high interest are 1) cyanide chemistry easily lends itself to a building-block approach and 2) the nature (ferromagnetic versus antiferromagnetic) of magnetic exchange interactions through a linear cyanide ligand is largely predictable.^[2–4] These attributes have inspired numerous research groups to pursue the synthesis of high-spin, magnetically anisotropic metal cyanide molecules with the goal of engendering slow paramagnetic relaxation of the magnetization, a phenomenon that has been likened to the behavior of single-domain particles. This “superparamagnetic-like” magnetic behavior of molecules, commonly referred to as “single-molecule magnetism”,^[5–11] has been observed for paramagnetic clusters that exhibit a large spin ground state combined with an appreciable degree of anisotropy (i.e., a negative zero-field splitting parameter D).^[5,6,10,11] Single-molecule magnet (SMM) behavior was first noted over ten years ago for an $\{\text{Mn}_{12}\}$ cluster of the oxide family,^[10,11] and many new examples of oxide-based SMMs have been prepared in the ensuing years.^[10,12] Progress in this area has been only incremental, however, in terms of raising the blocking temperature of the magnetization. One of the main reasons for this situation is that it is difficult to control the sign and magnitude of D . This limitation to realizing high-temperature SMMs is one of the focal points of research in the field.

One approach to increasing the magnetic anisotropy of paramagnetic clusters is to incorporate heavier transition elements, such as 5d metal ions, which exhibit strong spin-orbit coupling effects that can induce anisotropic magnetic-

exchange interactions.^[7,13–17] In this vein, we have been investigating the use of the paramagnetic Re^{II} anion complex $[\text{Re}^{\text{II}}(\text{triphos})(\text{CN})_3]^-$ (triphos = 1,1,1-tris(diphenylphosphanyl)methyl)ethane) as a building block for high nuclearity clusters with unusual magnetic properties.^[18] As a backdrop for these studies, we undertook a full investigation of the magnetic behavior and theoretical modeling of $[\text{Et}_4\text{N}][\text{Re}^{\text{II}}(\text{triphos})(\text{CN})_3]$, which revealed that the compound exhibits an unusually strong temperature-independent paramagnetism due to spin-orbit coupling of the $S = 1/2$ ground state and low-lying excited states.^[19–21] Given these intriguing findings, we proceeded to explore reactions of $[\text{Re}^{\text{II}}(\text{triphos})(\text{CN})_3]^-$ with complementary building blocks including MCl_2 reagents ($\text{M} = 3\text{d}$ metal ion). The results of these studies with Fe^{II} and Co^{II} chlorides are reported herein.

Single-crystal X-ray studies revealed the products to be distorted molecular cubes composed of both six- and four-coordinate vertices (Figure 1).^[22] The triphos ligands act as

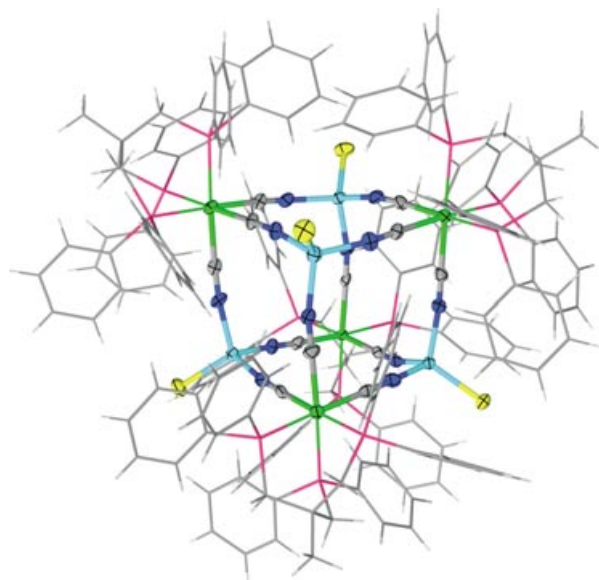


Figure 1. Thermal ellipsoid plot of $[\{\text{CoCl}\}_4\{\text{Re}(\text{triphos})(\text{CN})_3\}_4]$. Ellipsoids of the central core are drawn at the 50% probability level. The remaining atoms are depicted in stick mode for the sake of clarity.

facial-capping ligands for the Re^{II} centers, as expected, and a single chloride ligand completes the coordination spheres of the four 3d metal ions, which are in four-coordinate distorted tetrahedral environments. The steric demand of the triphos ligands, illustrated in the space filling diagrams in Figure 2, is clearly responsible for the lower coordination number of the Fe and Co centers in these compounds.^[23–25]

Relevant metal–ligand bond lengths and angles in $[\{\text{FeCl}\}_4\{\text{Re}(\text{triphos})(\text{CN})_3\}_4]$ (**1**) and $[\{\text{CoCl}\}_4\{\text{Re}(\text{triphos})(\text{CN})_3\}_4]$ (**2**) reveal subtle differences in the two molecular structures. The N–Fe–N angles in **1** range from $103.9(7)$ – $108.2(8)^\circ$ and the N–Fe–Cl angles range from $111.1(6)$ – $113.9(7)^\circ$. The N–Co–N angles in **2** are slightly more acute than those in **1**, ranging from $101.9(3)$ – $105.8(3)^\circ$; the N–Co–Cl angles are in the range $112.3(2)$ –

[*] E. J. Schelter, A. V. Prosvirin, K. R. Dunbar
Department of Chemistry
Texas A&M University
P.O. Box 30012, College Station, TX 77842-3012 (USA)
Fax: (+1) 979-845-7177
E-mail: dunbar@mail.chem.tamu.edu
W. M. Reiff
Department of Chemistry and Chemical Biology
Northeastern University
102 Hurtig Hall, 360 Huntington Ave., Boston, MA 02115 (USA)

[**] K. R. D. gratefully acknowledges the Department of Energy (DE-FG03-02ER45999), the National Science Foundation (NIRT-NSF DMR-0103455), the Welch Foundation A1449, and Texas A&M University (TITF) for funding of this research. The SMART CCD diffractometer and the SQUID magnetometer were purchased by funds provided by the National Science Foundation (Grants NSF-9807975 and NSF-9974899).

Supporting information for this article is available on the WWW under <http://www.angewandte.org> or from the author.

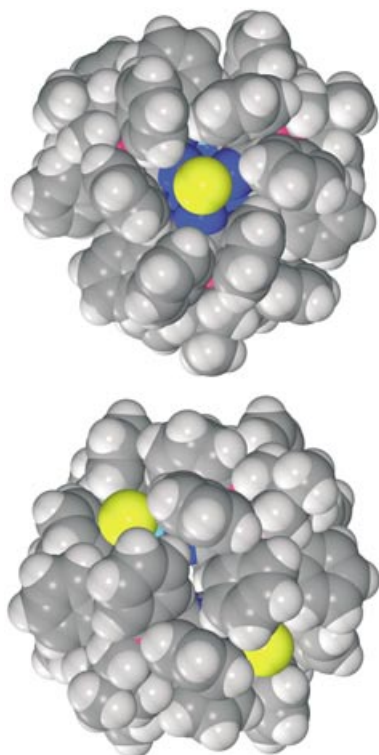


Figure 2. Space filling diagram for $[\{\text{CoCl}\}_4\{\text{Re}(\text{triphos})(\text{CN})_3\}_4]$ illustrating the high steric demand of the triphos ligands. Top: View along Fe–Cl vector (pseudo- C_3 -axis of cube). Bottom: Side view of cube face.

116.1(2)°. In both structures, the fact that the N–M–N angles are $> 90^\circ$ is compensated by deviations of the CN^- ligands from linearity (Re–C≡N angles range from 169.3(18)–177(2)° and 175.0(8)–179.3(10)°; M–N≡C angles range from 163.3(18)–174.3(16)° and 165.4(8)–174.1(8)° in **1** and **2** respectively).

Infrared spectroscopy performed on polycrystalline samples of **1** and **2** as Nujol mulls revealed the presence of two sharp, intense $\nu_{(\text{C}\equiv\text{N})}$ stretches located at 2011 and 1992 cm^{-1} in **1** and 2111 and 2096 cm^{-1} in **2**. The $\nu_{(\text{C}\equiv\text{N})}$ modes in **1** are shifted by -49 and -78 cm^{-1} from the starting material (2060, 2070 cm^{-1}),^[18] whereas the $\nu_{(\text{C}\equiv\text{N})}$ stretching bands in **2** are shifted by $+51$ and $+26$ cm^{-1} respectively. Typically, CN stretches shift to higher energies in going from a terminal to bridging mode, so it was initially puzzling that compound **1** exhibited anomalous behavior. These differences can be explained, however, on the basis of different oxidation states for the Re ion in **1** and **2**. Far-infrared spectroscopy performed on **1** revealed a feature at 354 cm^{-1} that is consistent with a $\nu_{\text{Fe–Cl}}$ stretching mode for a ferric iron, and Mössbauer spectra at 4, 77, and 298 K indicate the presence of a single iron species, namely a high-spin Fe^{III} nucleus ($\delta = 0.43$ mm s^{-1} and $\Delta E = 0.53$ mm s^{-1} , Figure 3). These data indicate that the Fe^{II} ions have become oxidized in the course of the reaction, and, since there are no counterions in the crystals of **1**, one must assign the oxidation state of Re in the cluster as Re^{I} . This conclusion is substantiated by the electrochemical properties of $[\text{Et}_4\text{N}][\text{Re}(\text{triphos})(\text{CN})_3]$ which reveal an accessible, reversible $\text{Re}^{\text{II}} \rightarrow \text{Re}^{\text{I}}$ reduction process at $E_{1/2} = -0.74$ V

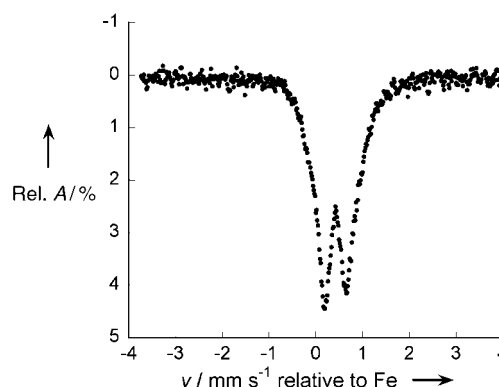


Figure 3. Mössbauer spectrum of $[\{\text{FeCl}\}_4\{\text{Re}(\text{triphos})(\text{CN})_3\}_4]$ at 77.5 K. The Quadrupole doublet indicates rapidly relaxing high-spin Fe^{III} center with $\delta = 0.43$ mm s^{-1} and $\Delta E = 0.53$ mm s^{-1} ; (Rel. A is the relative absorbance; v is velocity).

(dissolved in acetonitrile, versus Ag/AgCl).^[18] Moreover, there is a general contraction of Re–L bond lengths in **1** as compared to **2**, in accord with the presence of the Re^{I} ion, which can engage in stronger π -bonding interactions with the cyanide and phosphine ligands. The assignment of an $\text{Re}^{\text{I}}\text{–Fe}^{\text{III}}$ ground state is consistent with the shifted energies of the $\nu_{(\text{C}\equiv\text{N})}$ modes in the infrared spectra of the compounds, as it is well-known that these bands are sensitive to metal oxidation states.

Magnetization measurements were performed on **1** and **2** from $T = 2$ –300 K. The $\chi_m T$ versus T plot for **1** shows a room-temperature value of 14.72 emu K mol^{-1} (10.85 μ_B) and a low-temperature value of 1.45 emu K mol^{-1} (3.41 μ_B ; Figure 4).

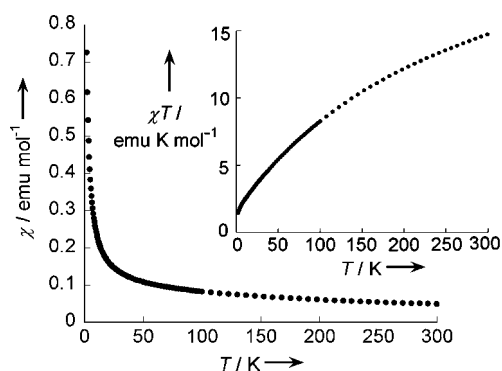


Figure 4. Temperature dependence of the magnetic susceptibility (χ_m) for $[\{\text{FeCl}\}_4\{\text{Re}(\text{triphos})(\text{CN})_3\}_4]$ (**1**). Inset shows $\chi_m T$ versus T .

The value of 14.72 emu K mol^{-1} is slightly low for four, non-interacting $S = 5/2$ Fe^{III} centers, (3.68 emu K mol^{-1} (5.43 μ_B) per Fe^{III} and low-spin, d^6 Re^{I} ions, which contribute only TIP).^[26] The calculated moment per Fe^{III} center continues to approach the spin-only value of 5.92 μ_B with increasing temperature, attaining a value of 5.60 μ_B at the limit of the experiment ≈ 350 K. Attempts to apply a simple model to the $\chi_m T$ versus T data that involved a combination of a small zero-field splitting parameter and weak next-nearest neighbor

interactions^[9] did not entirely reproduce the gradual slope of $\chi_m T$, but the data are reproducible for pure batches of crystals, thereby ruling out the presence of impurities. Further efforts are underway to develop a model for this system that accounts for the behavior of **1** over the entire temperature range.

In the case of compound **2**, the $\chi_m T$ versus T plot exhibits a high temperature product of 13.92 emu K mol⁻¹ (10.55 μ_B) and a low temperature product of 0.58 emu K mol⁻¹ (2.15 μ_B ; Figure 5). If the contribution of the Re^{II} centers at 300 K is

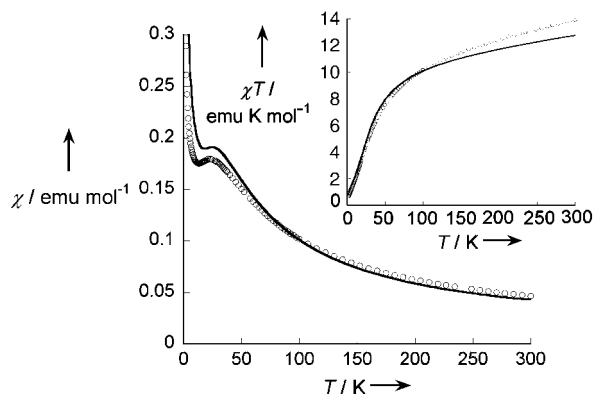


Figure 5. Temperature dependence of the magnetic susceptibility of $[\text{CoCl}_4][\text{Re}(\text{triphos})(\text{CN})_3]$ (**2**) and that of the model (solid line). Inset shows $\chi_m T$ vs T with that of the model (solid line). The model breaks down at higher temperatures due to the temperature dependence of the g value of the Co^{II} ions arising from zero-field splitting.

taken to be 0.63 emu K mol⁻¹ or 2.29 μ_B (the value of the parent compound $[\text{Et}_4\text{N}][\text{Re}(\text{triphos})(\text{CN})_3]$,^[18] one obtains a $\chi_m T$ value of 2.85 emu K mol⁻¹ (4.77 μ_B) for each Co^{II} ion, in accord with tetrahedral Co^{II} ($S=3/2$) and a typical orbital contribution.^[25] The χ_m versus T plot increases as the temperature is lowered until 21 K, after which temperature the value decreases before rapidly increasing again at 12 K. The $\chi_m T$ versus T data for **2** descends over the whole temperature range and approaches zero at low temperatures.

The magnetic data for **2** can be rationalized in terms of the well-described behavior of the 4A_2 ground state of the tetrahedral Co^{II} ion.^[27] Zero-field splitting of this ion ($\approx |7-15| \text{ cm}^{-1}$)^[27,28] leads to an effective spin $S'=1/2$ for the Co^{II} ion at low temperatures. The fact that both Re^{II} and Co^{II} ions in **2** are magnetically anisotropic poses a formidable challenge for the simulation of the magnetic behavior. A model for the magnetic susceptibility was developed by using MAGPACK (ANIMAG2),^[29] which accounts for the most influential factors on the susceptibility of **2**, namely, the zero-field splitting of the Co^{II} ions, the anisotropic g factors of the Co^{II} ions, and their anisotropic magnetic exchange. The data were reproduced by using an Ising exchange model and assumptions were made to limit the number of fitting parameters. The g values for the Re^{II} ion were set at $g_{\parallel}=2.4$ and $g_{\perp}=0.7$, values previously established by the $j-j$ coupling scheme developed for $[\text{Re}(\text{triphos})(\text{CN})_3]^-$.^[20] The best fit to the low-temperature data ($<40 \text{ K}$)^[30] was obtained for Co^{II} ion g values of $g'_{\parallel}=2.7$ and $g'_{\perp}=1.2$,^[31-34] $D_{\text{Co}}=-15 \text{ cm}^{-1}$ and $J_z=-5.5 \text{ cm}^{-1}$ (Figure 5).^[35] Most importantly, the model predicts

the maximum in χ_m vs T reasonably well. Additional work is currently underway to experimentally establish g and D values from EPR studies to further refine the model.

The results of this study demonstrate that the anion $[\text{Re}(\text{triphos})(\text{CN})_3]^-$ is a useful precursor for the high-yield self-assembly of unusual metal cyanide cubes in which four-coordinate pseudotetrahedral metal ions occupy four of the vertices of the cube along with the six-coordinate Re^{II} corners. The reaction with FeCl_2 led to a redox reaction to produce a cluster consisting of Re^I and high-spin Fe^{III} ions, a result that underscores the fact that choices of metal ions to combine with $[\text{Re}(\text{triphos})(\text{CN})_3]^-$ will need to be guided by a knowledge of their oxidation potentials. The combination of Re^{II} ($S=1/2$) and Co^{II} ($S=3/2$) in **2** leads to complex magnetic behavior dominated by the anisotropy of the ions as expected. In an effort to generalize this chemistry, we have also explored reactions of the divalent chlorides of Mn, Ni, Cu, Zn and crystallized analogous cubes in all cases. These preliminary results combined with the present studies constitute a family of homologous clusters whose comparative magnetic properties is expected to lend valuable insight into the parameters that affect the behavior, especially the large magnetic anisotropy of the Re^{II} ion.

Experimental Section

Synthesis of $[\text{FeCl}_4][\text{Re}(\text{triphos})(\text{CN})_3]$ (**1**): $[\text{Et}_4\text{N}][\text{Re}(\text{triphos})(\text{CN})_3]$ (0.080 g, 0.078 mmol) was dissolved in 5 mL of dry CH_3CN and treated with $\text{FeCl}_4(\text{thf})_6$ ^[36] (0.032 g, 0.034 mmol in 4 mL of CH_3CN and 1 mL of Et_2O) which produced a change from yellow to an intense blue. A crystalline blue sample was harvested after 18 h and washed with CH_3CN followed by Et_2O and air-dried. Yield: 0.053 g (63%). The synthesis of **2** (intense green) is identical to that of **1** except that the CH_3CN washings were minimized due to the higher solubility of **2** in CH_3CN . X-ray quality single crystals of **1** and **2** were obtained by layering CH_3CN solutions of the Re^{II} compound with $\text{CH}_3\text{CN}/\text{Et}_2\text{O}$ (9:1 v/v) solutions of MCl_2 . Elemental analysis calcd for **1**, $\text{C}_{176}\text{H}_{156}\text{N}_{12}\text{Cl}_4\text{P}_{12}\text{Fe}_4\text{Re}_4$: C 53.91, H 4.01, N 4.23, Cl 3.62; found: C 53.52, H 4.12, N 4.19, Cl 3.52. Elemental analysis calcd for **2**, $\text{C}_{176}\text{H}_{156}\text{N}_{12}\text{Cl}_4\text{P}_{12}\text{Co}_4\text{Re}_4$: C 53.74, H 4.00, N 4.27, Cl 3.61; found: C 53.89, H 4.16, N 4.12, Cl 3.58. IR (Nujol) for **1**: $\tilde{\nu}=2011, 1992 \text{ cm}^{-1}$ ($\text{C}\equiv\text{N}$); **2**: $\tilde{\nu}=2111, 2096 \text{ cm}^{-1}$ ($\text{C}\equiv\text{N}$). Mössbauer (77.5 K): **1**: $\delta=0.43 \text{ mms}^{-1}$ (relative to RT Fe), $\Delta E=0.53 \text{ mms}^{-1}$. DC magnetic susceptibility measurements were performed on microcrystalline samples of **1** and **2** with the use of a Quantum Design MPMS-2 SQUID magnetometer operating in the temperature range of 2–300 K at 0.1 T. Diamagnetic corrections were made with the use of Pascal's constants.

Received: May 10, 2004

Keywords: cage compounds · cluster compounds · cyanides · magnetic properties · rhenium

- [1] K. R. Dunbar, R. A. Heintz, *Prog. Inorg. Chem.* **1997**, 45, 283–391.
- [2] S. M. Holmes, G. S. Girolami, *J. Am. Chem. Soc.* **1999**, 121, 5593–5594.
- [3] W. R. Entley, G. S. Girolami, *Science* **1995**, 268, 397–400.
- [4] T. Mallah, S. Thiebaut, M. Verdaguer, P. Veillet, *Science* **1993**, 262, 1554–1557.

- [5] C. P. Berlinguette, D. Vaughn, C. Canada-Vilalta, J. R. Galan-Mascaros, K. R. Dunbar, *Angew. Chem.* **2003**, *115*, 1561–1564; *Angew. Chem. Int. Ed.* **2003**, *42*, 1523–1526.
- [6] J. J. Sokol, A. G. Hee, J. R. Long, *J. Am. Chem. Soc.* **2002**, *124*, 7656–7657.
- [7] F. Bonadio, M. Gross, H. Stoeckli-Evans, S. Decurtins, *Inorg. Chem.* **2002**, *41*, 5891–5896.
- [8] Z. J. Zhong, H. Seino, Y. Mizobe, M. Hidai, A. Fujishima, S. i. Ohkoshi, K. Hashimoto, *J. Am. Chem. Soc.* **2000**, *122*, 2952–2953.
- [9] V. Marvaud, C. Decroix, A. Scullier, F. Tuyeras, C. Guyard-Duhayon, J. Vaissermann, M. Marrot, F. Gonnet, M. Verdager, *Chem. Eur. J.* **2003**, *9*, 1692–1705.
- [10] D. Gatteschi, R. Sessoli, *Angew. Chem.* **2003**, *115*, 278–309; *Angew. Chem. Int. Ed.* **2003**, *42*, 268–297.
- [11] R. Sessoli, H. L. Tsai, A. R. Schake, S. Wang, J. B. Vincent, K. Folting, D. Gatteschi, G. Christou, D. N. Hendrickson, *J. Am. Chem. Soc.* **1993**, *115*, 1804–1816.
- [12] A. J. Tasiopoulos, A. Vinslava, W. Wernsdorfer, K. A. Abboud, G. Christou, *Angew. Chem.* **2004**, *116*, 2169–2173; *Angew. Chem. Int. Ed.* **2004**, *43*, 2117–2121.
- [13] O. Kahn, J. Larionova, L. Ouahab, *Chem. Commun.* **1999**, 945–952.
- [14] V. S. Mironov, L. F. Chibotaru, A. Ceulemans, *J. Am. Chem. Soc.* **2003**, *125*, 9750–9760.
- [15] S. Tanase, F. Tuna, P. Guionneau, T. Maris, G. Rombaut, C. Mathoniere, M. Andruh, O. Kahn, J. P. Sutter, *Inorg. Chem.* **2003**, *42*, 1625–1631.
- [16] R. Podgajny, C. Desplanches, B. Sieklucka, R. Sessoli, V. Villar, C. Paulsen, W. Wernsdorfer, Y. Dromzee, M. Verdager, *Inorg. Chem.* **2002**, *41*, 1323–1327.
- [17] J. Larionova, R. Clerac, B. Donnadieu, S. Willemin, C. Guerin, *Cryst. Growth Des.* **2003**, *3*, 267–272.
- [18] E. J. Schelter, J. K. Bera, J. Bacsá, J. R. Galan-Mascaros, K. R. Dunbar, *Inorg. Chem.* **2003**, *42*, 4256–4258.
- [19] K. R. Dunbar, E. J. Schelter, B. S. Tsukerblat, S. M. Ostrovsky, V. Y. Mirovitsky, A. V. Palii, *Polyhedron* **2003**, *22*, 2545–2556.
- [20] K. R. Dunbar, E. J. Schelter, A. V. Palii, S. M. Ostrovsky, V. Y. Mirovitskii, J. M. Hudson, M. A. Omary, S. I. Klokishner, B. S. Tsukerblat, *J. Phys. Chem. A* **2003**, *107*, 11102–11111.
- [21] K. R. Dunbar, E. J. Schelter, B. S. Tsukerblat, A. V. Palii, S. M. Ostrovsky, V. Y. Mirovitskii, S. I. Klokishner, *Adv. Quantum Chem.* **2003**, *44*, 413–428.
- [22] Crystal data for $[\text{FeCl}]_4[\text{Re}(\text{triphos})(\text{CN})_3]_4 \cdot 6.5 \text{CH}_3\text{CN}$ (**1**): $\text{C}_{189}\text{H}_{174.75}\text{Cl}_4\text{Fe}_4\text{N}_{18.50}\text{P}_{12}\text{Re}_4$, $M_r = 4186.86$, monoclinic, $C2/c$ (No. 15), $a = 66.829(19)$, $b = 18.811(5)$, $c = 32.575(9)$ Å, $\beta = 106.957(8)^\circ$, $V = 39170(19)$ Å³, $Z = 8$, $\rho_{\text{calc}} = 1.420 \text{ g cm}^{-3}$, $\mu = 2.954 \text{ mm}^{-1}$, 94524 reflections (33330 unique) to $2\theta = 49.42^\circ$, 1831 variables, $R = 0.1258$, $wR(F_o^2) = 0.2838$ [19686 data, $I > 2\sigma(I)$], $\text{GooF} = 1.108$. Crystal data for $[\text{CoCl}]_4[\text{Re}(\text{triphos})(\text{CN})_3]_4 \cdot 8.5 \text{CH}_3\text{CN} \cdot 0.5 \text{THF}$ (**2**): $\text{C}_{195}\text{H}_{184.75}\text{Cl}_4\text{Co}_4\text{N}_{20.50}\text{O}_{0.50}\text{P}_{12}\text{Re}_4$, $M_r = 4317.34$, monoclinic, $C2/c$ (No. 15), $a = 66.803(13)$, $b = 18.839(4)$, $c = 32.491(7)$ Å, $\beta = 106.62(3)^\circ$, $V = 39182(14)$ Å³, $Z = 8$, $\rho_{\text{calc}} = 1.464 \text{ g cm}^{-3}$, $\mu = 2.998 \text{ mm}^{-1}$, 141634 reflections (33382 unique) to $2\theta = 49.42^\circ$, 2089 variables, $R = 0.0648$, $wR(F_o^2) = 0.1520$ [27521 data, $I > 2\sigma(I)$], $\text{GooF} = 1.180$. X-ray data were measured at 110(2) K on a Siemens SMART CCD diffractometer with graphite monochromated $\text{MoK}\alpha$ ($\lambda_\alpha = 0.71073$ Å) radiation. Structures **1** and **2** were solved and refined using SHELX97 (G. M. Sheldrick, SHELXL97, Program for the Refinement of Crystal Structures, University of Göttingen, Germany, 1997) with the graphical interface X-SEED (L. J. Barbour, X-Seed, Graphical interface to SHELX-97 and POV-Ray, 1999). CCDC 241395 & 241396 (**1** and **2**) contain the supplementary crystallographic data for this paper. These data can be obtained free of charge via www.ccdc.cam.ac.uk/conts/retrieving.html (or from the Cambridge Crystallographic Data Centre, 12 Union Road, Cambridge CB2 1EZ, UK; fax: (+44) 1223-336-033; or deposit@ccdc.cam.ac.uk).
- [23] N. G. Connelly, O. M. Hicks, G. R. Lewis, A. G. Orpen, A. J. Wood, *Dalton* **2000**, 1637–1643.
- [24] V. Jacob, S. Mann, G. Huttner, O. Walter, L. Zsolnai, E. Kaifer, P. Rutsch, P. Kircher, E. Bill, *Eur. J. Inorg. Chem.* **2001**, 2625–2640.
- [25] M. Fritz, D. Rieger, E. Baer, G. Beck, J. Fuchs, G. Holzmann, W. P. Fehlhammer, *Inorg. Chim. Acta* **1992**, *198–200*, 513–526.
- [26] F. A. Cotton, G. Wilkinson, M. Bochmann, C. Murillo, *Advanced Inorganic Chemistry*, 6th ed., Wiley, New York **1998**.
- [27] R. L. Carlin, *Science* **1985**, *227*, 1291–1295.
- [28] J. Krzystek, S. A. Zvyagin, A. Ozarowski, A. T. Fiedler, T. C. Brunold, J. Telser, *J. Am. Chem. Soc.* **2004**, *126*, 2148–2155.
- [29] J. J. Borrás-Almenar, J. M. Clemente-Juan, E. Coronado, B. S. Tsukerblat, *J. Comput. Chem.* **2001**, *22*, 985–991.
- [30] At higher temperatures the system can no longer be treated as an effective spin $S' = 1/2$, and the population of excited states is expected to lead to very different g values for the Co^{II} ion.
- [31] R. P. Stapele, H. G. Beljers, P. F. Bongers, H. Zijlstra, *J. Chem. Phys.* **1965**, *44*, 3719–3725.
- [32] H. G. Beljers, P. F. Bongers, R. P. van Stapele, H. Zijlstra, *Phys. Lett.* **1964**, *12*, 81–82.
- [33] N. Pelletier-Allard, *C. R. Hebd. Seances Acad. Sci.* **1964**, *258*, 1215–1218.
- [34] N. Pelletier-Allard, *C. R. Hebd. Seances Acad. Sci.* **1964**, *259*, 2999–3002.
- [35] Plots of the model of the temperature dependent anisotropic susceptibilities of **2** are provided as supporting information.
- [36] H. Zhao, R. Clerac, J. S. Sun, X. Ouyang, J. M. Clemente-Juan, C. J. Gomez-Garcia, E. Coronado, K. R. Dunbar, *J. Solid State Chem.* **2001**, *159*, 281–292.